ORNL/TM-2024/3613

Studies of Helium Behavior in Uranium Hexafluoride

Jason M. Richards
Lee D. Trowbridge
Harold Jennings
Tara A. Davis
Michael Singleton
Glenn A. Fugate

September 2024

OAK RIDGE National Laboratory

ORNL IS MANAGED BY UT-BATTELLE LLC FOR THE US DEPARTMENT OF ENERGY

ORNL/TM-2024/3613

Nuclear Nonproliferation Division

STUDIES OF HELIUM BEHAVIOR IN URANIUM HEXAFLUORIDE

Jason M. Richards*
Lee D. Trowbridge*
Harold Jennings*
Tara A. Davis*
Michael Singleton†
Glenn A. Fugate‡

* Oak Ridge National Laboratory
† Lawrence Livermore National Laboratory
‡ Pacific Northwest National Laboratory

September 2024

Prepared by
OAK RIDGE NATIONAL LABORATORY
Oak Ridge, TN 37831
managed by
UT-BATTELLE LLC
for the
US DEPARTMENT OF ENERGY
under contract DE-AC05-00OR22725

CONTENTS

LIST OF FIGURES

LIST OF TABLES

ABSTRACT

Several issues have arisen from experimental observations and/or theoretical postulation related to the behavior of helium in uranium hexafluoride (UF_6) matrices and how it may impact the ability to use this noble gas to quantify the fill date of the cylinder. A series of experiments was conducted to address several such issues, and the results and implications are reported here.

Two issues relate to bias in the helium measurement due to ambient air from extraneous sources such as atmospheric air or from potential holdup in a large, activated alumina chemical trap. These issues are really a question of differential retention of helium versus three other inert gas isotopes (representative of other noble gases found in air) used as a calibration for air in leakage. Discernable bias was not detected in either case.

Another issue had to do with helium potentially brought into the cylinder by a liquid UF_6 fill and subsequently released as the material solidifies and/or during storage. The solubility of helium in liquid UF_6 was measured to investigate this theory. The experiment quantified the potential magnitude of the initial helium contribution if present.

The final issue was that of retention of helium in solid UF_6. Investigation of this theory necessitated quantifying both the solubility and the diffusivity of helium in UF_6. In one experiment, the solubility was measured at cryogenic temperature, allowing quantification of helium in solid UF_6 such as would be found in a cold trap. In a second experiment, transport of helium into and through a macroscopic plug of solid UF_6 was examined. The transport was very slight although apparently detectible. Effectively, only an upper limit to the transport could be determined, but that limit implied that helium holdup in solid UF_6 is a real possibility.

1. INTRODUCTION

The headspace measurement process has been shown to be viable for small, aged uranium hexafluoride (UF_6) containers, especially those with higher assays, which generate relatively more ^4He through alpha radioactive decay (Singleton, Beaumont and Cassata) (J Richards). In extending this technique to larger cylinders and lower ^{235}U assays, some specific concerns have arisen both conceptually and experimentally (Singleton, Stephenson and Beaumont). Sample cylinders in this work have tended to be filled under well-controlled laboratory practices that include burping of parent cylinders, thorough water removal processes, and use of medium vacuum conditions (~10^{-5} psia). Industrial-scale cylinders used in accordance with common industrial practices can be assumed to have less stringent requirements, including being evacuated to less than 3 psia (SJ Hansen) to 5 (USEC) psia. (It is important to note that the specification has changed with time and may have been even higher in the past.) Lower-assay cylinders generate less ^4He per unit mass of UF_6. Additionally, little information is available to allow comparison of helium or other noble gas behavior between small-scale cylinders and the significantly thicker UF_6 solids of industrial cylinders. Thus, a given absolute uncertainty in helium measurement yields a larger absolute uncertainty in age. These behaviors need to be studied to ensure that the capability as developed on sample cylinders can be applied to industrial-scale cylinders.

1.1 AIR

Because of these uncertainty concerns, measurements on large cylinders may be more vulnerable to biases caused by other sources of helium within the cylinder. From the start of the project, the mass spectrometry measurements of ^4He have also measured several other noble gas isotopes (e.g., ^{36}Ar, ^{38}Ar, ^{84}Kr) to assess sample contamination from air (Singleton, Beaumont and Cassata). Observation of those

isotopes in the naturally occurring ratios to one another is taken as an indication of contamination with atmospheric air. Helium-4 in the background helium content from the potential air inside the cylinder was quantified using the ratioing of ^{4}He to one of the other noble gases in ambient air. The determined background contribution is then subtracted from the measured quantity to determine the helium from radioactive decay. The natural ratio to the above three isotopes is then subtracted from the total ^{4}He measured in the processed gas sample. This approach has worked well for the small cylinders studied in this work and should remove bias from added atmospheric air whatever its source (e.g., air present in the cylinder headspace, residual air in the sampling and processing manifold, air used in the mass spectrometric measurement process itself).

1.2 OTHER POTENTIAL SOURCES OF HELIUM

Several other potential sources of bias have been postulated, and this report describes four experiments designed to quantify those biases.

- **Solubility of helium in solid UF_6** – It is likely that any helium still dissolved in the solid will not immediately be available for collection when the headspace is sampled. Typically, multiple samples are collected, which allows the use of serial dilution to estimate the headspace volume. Any helium in the solid UF_6 may transfer to the headspace at a currently unknown rate, producing an elevated concentration compared to the decreased concentration expected from the serial dilution. This experiment attempted to quantify the helium in solid UF_6.

- **Solubility of helium in liquid UF_6** – In some cases, the transfer to a cylinder is performed using UF_6 in the liquid state. Any helium dissolved in the liquid will transfer to the destination cylinder, providing an initial, unaccounted for contribution. This experiment sought to determine the saturation level as a solubility constant for helium in liquid UF_6 to provide an upper boundary of what may initially be present within the cylinder.

- **Diffusivity of helium in solid UF_6** – This experiment sought to measure the rate of transport of ^{4}He into and through solid UF_6 to answer the question of how rapidly helium can permeate the gas phase and solid UF_6.

- **Atmospheric helium** bias due to processing – This experiment examined the possibility of bias in the measurement of helium as a ratio to other noble gases that might result from one of several conditions inherent in the age dating process. Several experiments were conducted in an attempt to observe bias in the helium measurements for the postulated conditions.

Experiments addressing the above four areas are described and discussed in the sections that follow. In a few cases, more elaborate discussion was considered warranted and is included in Appendixes A and B.

2. SOLUBILITY OF HELIUM IN SOLID UF_6

Transport of a gas through a permeable solid depends on the solubility of the gas in the solid (helium through solid UF_6, in this case) and is typically a function of the partial pressure of that gas outside the solid and the diffusivity of the gas within that solid. *Solubility* is of importance for the age dating method because ^{4}He dissolved in the solid may not be immediately available for measurement during the brief period in which the headspace gas is sampled, even if the helium is in equilibrium between the gas and solid phases. *Diffusivity* is important because this approach assumes any helium generated in the solid UF_6 by alpha decay must diffuse to the surface of the solid and substantially equilibrate into the gas phase. Low diffusivity can create a bias because the helium in the headspace will be lower than expected,

thereby making the derived age low. To date, the project has assumed the permeation rate of helium is fast (potentially fast enough to overcome solubility) or that the solubility is low.

While aware of this potential issue, the project had not explicitly addressed it. Within the uncertainty of the measurements and experimental techniques, loss of helium to solubility was not observed in the small cylinders examined early in the project, meaning the loss, if any, was less than 10% (Singleton, Beaumont and Cassata).

Although empirically the age dating process has generally worked for small cylinders (i.e., 1S, 2S, and laboratory cylinders of similar dimensions), it was not known whether this issue would become significant in industrial cylinders, which have considerably larger UF_6 solid deposits. The main concern is the difference in the distance an alpha decay may have to travel through solid UF_6 in a sample cylinder compared to an industrial-scale cylinder.

2.1 EXPERIMENTAL APPROACH FOR HELIUM SOLUBILITY IN SOLID UF_6

An experiment was conducted with the intent of producing solid UF_6 saturated in helium. The experiment was done under a known helium partial pressure, thereby determining the solubility of the gas in solid UF_6 for that one set of conditions.

The apparatus employed two U-tubes in series as shown in Figure 1. The first U-tube was initially filled with 220 g solid UF_6. It was condensed out of the gas phase under flowing conditions to ensure the vessel was not plugged. The solid-containing U-tube was allowed to reach ambient temperature while the second U-tube was chilled. A carrier gas of 100 Torr helium was circulated using a metal bellows such that it flowed through the loaded U-tube and through the chilled U-tube, which should have transferred UF_6 gas from the loaded to the chilled tube where it should have frozen. The initial experiment chilled the second U-tube with an ethanol/ethylene glycol and dry ice mixture to a temperature commonly employed with large-scale industrial processes (typically –40°C), but the second U-tube formed a plug. The experiment was performed a second time using liquid nitrogen (LN_2) (−196°C), which is commonly used in laboratory-scale work. The concentration of UF_6 in the gas phase was monitored by infrared spectroscopy using the very strong 625 cm^{-1} band with the transfer being declared complete when this infrared band could no longer be observed (~0.001 Torr partial pressure). At this point the system underwent a flushing process as quickly as possible while maintaining the "loaded" U-tube at LN_2 temperature. This process involved evacuation to less than 1 Torr followed by flushing the system with ultrahigh-purity nitrogen to 100 Torr. This process was repeated three times before filling the system to 100 Torr of ultrahigh-purity nitrogen. Some potential for helium loss exists during the flushing process because the incoming nitrogen gas could impart some energy to the chilled solid, thereby allowing for premature sublimation and release of helium trapped near the surface of the UF_6 solid. The U-tube was immersed 1 to 2 in. deeper in LN_2 during flushing, and the process was done as quickly as possible to minimize the potential losses. The U-tube that contained solid UF_6 (loaded under 100 Torr of helium) was isolated and allowed to warm to ambient temperature, and the now-empty U-tube was chilled using an LN_2 bath. A carrier gas of ultrahigh-purity nitrogen was added to the manifold and allowed to circulate for 10 min to reach equilibrium before a sample was collected. A flow was then established to transfer the UF_6 from the loaded U-tube to the initial empty U-tube under nitrogen. The experiment was monitored by FTIR spectroscopy and stopped once all UF_6 had been transferred. The gas was then sampled after the transfer.

The design of this experiment was to allow helium to be incorporated into the UF_6 condensing into the second U-tube, letting it reach its solubility at 100 Torr partial pressure and –196°C (equivalent to 77 K or perhaps a somewhat higher due to thermal gradients). Once all UF_6 had transferred back to the first U-tube, the gas flow was stopped, and the carrier gas was sampled by expansion of a small known

percentage into an evacuated cylinder. Both sample cylinders were then measured by variable-inlet mass spectrometer (VIMS) for total helium content.

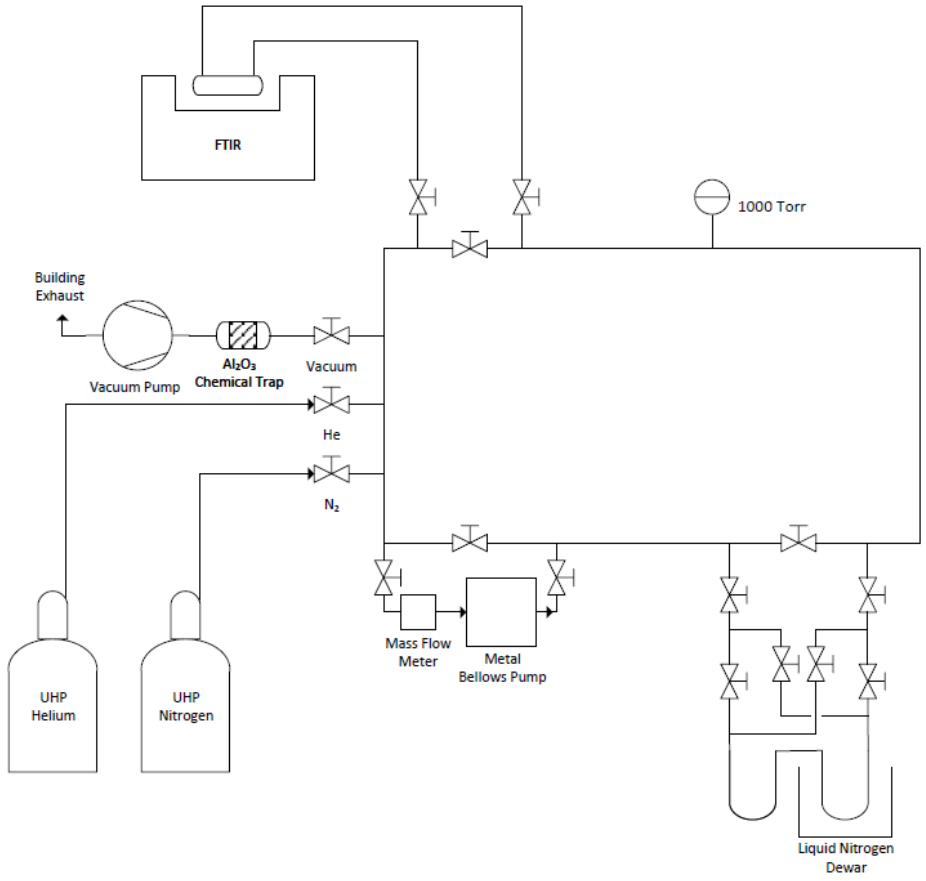

Figure 1. The manifold configuration for helium studies in solid UF_6.

2.2 RESULTS FOR HELIUM SOLUBILITY IN SOLID UF_6

Ideally, the first sample should contain only residual helium not removed from the system by evacuation and flushing with nitrogen and serve as background for the second sample. The second sample should contain any gas that was released from the 100 Torr helium-saturated solid during the second transfer. The total helium content of the samples was measured by a VIMS equipped with an inlet getter (to chemically remove any gases except noble gases). The measured helium content of the sample cylinders was then used to calculate the helium content in the carrier gas before and after the second transfer. The difference between the helium content of the carrier gas before and after the second transfer was assumed to be the helium dissolved in the UF_6 solid during the first transfer. The first ("residual") sample was calculated to be 4.5 mTorr in 931 cc manifold volume, while the second sample was calculated to be 7.0 mTorr of helium in 952 cc manifold volume (volume change includes volume of one or both samples). After applying a small correction for the helium removed during the collection of the first sample and assuming the residual helium pressure was the same throughout the manifold, the dissolved helium was calculated to comprise 42% of the total helium found.

This result suggests that measurement of helium in solid UF_6 yielded a mole ratio of helium to UF_6 of 2.6×10^{-6} at the specific conditions of 77 K and 100 Torr partial pressure helium.

A common and useful approximation to the behavior of solubility is Henry's law, which essentially states that at equilibrium the concentration of a gas dissolved within a solid is proportional to the concentration of that gas in the void space in contact with that solid. That ratio is the solubility constant. With appropriate unit conversion, one form of Henry's law yields the dimensionless solubility constant H^{CC}, which can be expressed as

$$H^{CC} = \frac{C_{SOLID}}{C_{GAS}},$$

where C_{SOLID} and C_{GAS} are the concentrations, in the same units (e.g., moles/cc), of the dissolved gas in the solid and the same species in the gas phase. (Note that C_{GAS} was calculated using the ideal gas law [n/V = P/RT, where *n* is moles, *V* is volume, *P* is pressure, *T* is temperature, and *R* is the ideal gas constant], which has an inherent temperature dependence.) There are inherent assumptions that the gas is in contact with the solid with and that the system is in thermodynamic equilibrium with the solid. In these terms, the mole ratio listed above yields a value of 0.223% for H^{CC} at 77 K.

The values of H^{CC} are specific to each pair of species in the gas and condensed phases but are (per Henry's law) independent of pressure. The value will, however, vary with temperature. The effective temperature at which the bulk of the UF_6 freezing takes place is uncertain and could be as high as 190 K. (See discussion in Sect. 2.3.) If that temperature were the operative one, the value of H^{CC} at 190 K would be 0.500%. A value at room temperature is also of interest, and a likely (but partially subjectively chosen) value for H^{CC} at room temperature is 0.600%.

This value follows from the above 77 K value, and the results of the room temperature helium diffusivity experiment are discussed later in this report. Details are provided in APPENDIX B.

2.3 DISCUSSION FOR HELIUM SOLUBILITY IN SOLID UF_6

In a UF_6 cylinder, the solubility of helium in the solid UF_6, assuming the system is equilibrated between the gas in the headspace and that dissolved in the solid, will have only a minor effect on the age dating result compared to typical errors reported for the process. The largest effect will come when the cylinder has the maximum quantity of UF_6. Practically speaking, UF_6 cylinders are limited to being nearly full as a liquid. (SJ Hansen). This maximum comes for "full cylinders," which, in UF_6 handling parlance, are ones that are nearly full when the UF_6 is in liquid form. Because of the large increase in density upon freezing, a full cylinder cooled to room temperature will have only about 60% of its volume occupied by solid UF_6 with the remaining "headspace" being occupied by only gas. At equilibrium, if the cylinder contains "X" × 40% units of helium in the gas phase, it will also contain "X" × 60% × H^{CC} units of helium dissolved in the solid. At equilibrium, the solid will thus contain the following fractions of the helium in the cylinder: 0.3% (if using the 77 K solubility value) or 0.9% (if using the 23°C estimate for H^{CC}). The age dating measurement will be biased low by these percentages, but that bias is within the expected uncertainty of the measurement technique, which is typically on the order of 10–20% (Singleton, Beaumont and Cassata).

None of the above should be interpreted to imply that helium formed within the solid by radioactive decay will necessarily rapidly equilibrate by diffusion with the gas phase. The assumption of equilibrium between radiogenic gas and bulk solid has yet to be addressed experimentally. However, 1S-type containers containing approximately 400 g of UF_6 have been found to be at or near equilibrium when radiogenic helium was measured a few months to a few years after filling. While the solid may not have

high diffusivity, it does have very low fracture toughness and readily fractures during thermal cycling within a few degrees.

There are several uncertainties in the measurement and therefore also in the solubility value derived. One relates to the effective temperature of the measurement, which has been taken as being 77 K, the LN_2 boiling point. But the cold trap is a dynamic system, so the actual temperature at which the desublimation of UF_6 occurs should be higher than that due to thermal loads (heat of sublimation and heat capacity of inflowing gas) and thermal conductivity (from the surface of the solid UF_6 to the U-tube wall to the LN_2). Some of the trapped UF_6 will be deposited where the U-tube is sufficiently chilled to reduce the UF_6 vapor pressure to near zero, even if it is somewhat above the level of the LN_2 coolant. Likely deposition of UF_6 and consequent dissolution of helium will occur over a range of temperatures above 77 K. If we took the maximum freezing temperature to be 190 K (very much higher and UF_6 would have been detected by the infrared spectrometer), the calculated value of H^{CC} would rise to 0.5%. That approach does not answer the uncertainty due to this effect but at least limits it.

The method of clearing the experimental system of the initial 100 Torr helium followed common practice but might have led to some discrepancies. There were four evacuations, each of 99% or more of the system gas, and three fills with nitrogen. If each fill perfectly mixed with residual gas from the prior evacuation, residual helium should have gone down by eight orders of magnitude to 1 μTorr from its initial 100 Torr. Measurement of the final gas composition, however, showed helium at 4.5 mTorr. This could easily be due to imperfect mixing, but it also conceivably might be due to evolution of some helium from the UF_6 deposit. If that waas the case, we would need to count the residual as part of the dissolved helium. In that case, the listed solubility would be more of a lower limit on the actual value of the solubility.

In the experimental technique used here, it is assumed that the second UF_6 transfer liberates all dissolved helium to the gas phase, but some helium will be dissolved in the desublimed first U-tube. The level of helium measured in the gas after the second transfer was on the order of 1×10^{-4} mTorr, six orders of magnitude below the initial 100 Torr helium partial pressure employed at the beginning of the experiment. Per Henry's law, the dissolved helium should in the final step and therefore also be six orders of magnitude lower, a completely inconsequential loss.

Additionally, it should be noted that there is an inherent assumption about the rate of the permeability of helium in solid UF_6. This rate will depend on several things, potentially including the temperature of the system, the thickness of the solid through which the gas must move to reach the solid–gas interface, and the properties of the solid phase(s). The deposit on the wall of the U-tube was thin, potentially allowing some of the helium to have been lost during the flushing stages of the experiment. This rate may be as important as the solubility of helium in the solid because rapid transfer (i.e., minutes to reach equilibrium) to the gas phase could negate even high solubility. Aspects of this potential impact will be covered in Sect. 4.

3. SOLUBILITY OF HELIUM IN LIQUID UF_6

The age dating process does not directly involve UF_6 melting, but in industrial handling of UF_6, especially historically, handling or transfer in the liquid form has often been employed. This approach also assumes that the headspace is not burped after a liquid-filled cylinder has been allowed to cool and form solid UF_6, so any helium carried into the vessel will be in place when accessed for sampling. Therefore, it was desirable to know how that might affect helium disposition in a gas-liquid system. For that reason, an experiment was performed to determine the solubility of helium in liquid UF_6 that could, for example, govern the amount of initially present helium that would remain after a liquid transfer.

3.1 EXPERIMENTAL APPROACH

A double-valved 75.2 cc vessel with 86.7 g UF_6 was used in this study. The vessel was chilled to LN_2 temperature to reduce the vapor pressure before evacuation to sub-mTorr levels. At this temperature, the solid volume UF_6 occupies at LN_2 temperatures can be calculated as 13.96 cc or 16.10% using reported densities (JC Anderson). The headspace was filled with 100 Torr helium, and the cylinder was isolated. While the addition of the helium took fewer than 5 s, some of the ambient-temperature gas might have cooled when it contacted the LN_2-cooled UF_6 solid and/or vessel base and side walls. Because the pressure (and ultimately the mass or moles) of the gas is dependent upon temperature, the variable pressure is a source of error as the quantity of helium added is uncertain due to the temperature variation along the height of the bottle. Colder regions will have helium at higher densities than warmer regions. For purposes of analysis, it was assumed that the helium was added to the cylinder at 22°C. Although this assumption was reasonable given the transfer was done quickly, it likely led to an underestimation of the quantity added.

The bottle was then warmed to 100°C to liquefy the UF_6 and inverted several times to provide good contact and mixing between the liquid UF_6 and the helium gas. The vessel was then held at 100°C for 1 h to allow equilibration of the helium between the headspace and the liquid. The condition of the cylinder at that time (before any sampling) was calculated to be 100°C, 75.2 cc total volume, 86.7 g UF_6, 24.9 cc UF_6 liquid volume (JC Anderson), and 50.3 cc headspace (calculated as the difference between the total and gas volumes). The bottle was inverted for sampling, and the entire system was isothermal. This approach should have completely filled the 2.2 cc bottle with liquid UF_6 without headspace gas. Unfortunately, the initial 2.2 cc sample was taken from the liquid but was compromised in follow-on processing, but a second 2 cc liquid sample was taken and successfully analyzed.

For purposes of analysis, it was assumed that no additional equilibration of helium between gas and liquid phase occurred after the initial mixing. The second 2.2 cc sample was calculated to contain 7.495 g UF_6 (21.29 mmol UF_6), which represents 9.5% of the total liquid UF_6 originally in the cylinder.

This small liquid sample was expanded into an evacuated receiving manifold that had sufficient volume to allow all sampled UF_6 to evaporate into the gas phase, thus liberating its dissolved helium. A small portion of this manifold was chilled with LN_2 to solidify the UF_6. A known fraction of the residual gas from the sampling manifold was then measured for helium content using the VIMS. This measurement yielded a value of 0.445 µmol helium. The mole ratio for the 2.2 cc sample can therefore be calculated to be 20.9 µmol helium per mol UF_6. This value is taken to be the original mole ratio in the bottle at the time of sampling.

The gas-phase concentration of helium in the bottle prior to sampling can be calculated using the following logic. First, the entire original liquid phase is assumed to have the helium-to-UF_6 mole ratio listed above. The gas phase must contain the remainder of the helium originally added (at 22°C). Initial (room temperature) and final (100°C) physical conditions and partitioning parameters are listed in Table 1. Under these assumptions, H^{CC} for helium in liquid UF_6 at 100°C is computed to be 3.10%.

Table 1. Physical properties and partitioning parameters for helium in liquid UF_6 solubility experiment

	Original fill		Liquid sampling		Totals
	Gas	Solid	Gas	Liquid	
Volume (cc)	61.2	14.0	50.3	24.9	75.2
T (°C)	22	–196 (77 K)	100	100	
UF_6 den g/cc*	0.000	6.211	0.0347	3.407	
UF_6 (mol)	0.000	0.2461	0.0050	0.2414	0.2464
P (Torr helium)	100		152		
n (mol helium)	3.33×10^{-4}	0	3.28×10^{-4}	5.04×10^{-6}	
Solubility-mol ratio (He/UF_6)			2.09×10^{-5} @ 100°C/152 Torr helium		
H^{CC}			3.10% @ 100°C/152 Torr helium		

*Densities of gas and liquid UF_6 taken from reference equations (JC Anderson).

3.2 DISCUSSION OF HELIUM SOLUBILITY IN LIQUID UF_6

The liquid solubility of helium in UF_6 is approximately an order of magnitude higher than the solid solubility, although it should be noted that the two measurements are made at greatly different temperatures. Thus, some of the solubility difference can be attributed to the difference between solid and liquid-phase behavior and some simply to the temperature difference.

Interestingly, this helium solubility value in liquid UF_6 falls within the range as H^{CC} values for helium in a variety of common liquid organics. (See discussion in APPENDIX A.)

The solubility of helium in liquid UF_6 should have no direct effect on bias in age dating measurements because the melting is not part of the protocol. However, it could indirectly affect how much helium is present at the original time of fill if the cylinder is filled with liquid UF_6, and the liquid contained an initial burden of helium. The actual effect is difficult to quantify because it depends on the specific operations within the facility, which are often unknown and can be prone to change over time and even from operator to operator during shift work. One also must speculate on the quantities of helium that could be present during different fill operations. Generally, the operation accumulates UF_6 in a condenser (referred to as “cold trap” or by other terminology) where material is frozen from the gas phase. The size and orientation are subject to facility design concerns such as space, cooling and heating mechanism, criticality safety, or other issues. Helium is likely to collect in these vessels from alpha decay events within the UF_6 or from holdup (also known as “heels” or “solids” or by other names). Additionally, facilities may have other sources of helium including leak-check sensors, certain welding applications, or a light gas contaminant during enrichment or conversion. The general conclusion is that the level of variability during filling is likely bound by this value for liquid-filled cylinders and would be considered part of the error in the method.

4. DIFFUSIVITY OF HELIUM IN SOLID UF_6

At the basis of the helium age dating forces for old UF_6 cylinders is the question of whether helium embedded in solid UF_6 (created there by alpha decay of uranium or daughter isotopes) can be usefully measured in the gas in the cylinder’s headspace. Factors influencing this question include (a) the solubility of helium in solid UF_6 and (b) the diffusivity of helium in solid UF_6. Age dating experiments

have been conducted on small-scale containers with promising results although without directly addressing these questions. As attention began to focus on larger cylinders, these questions became more important because larger cylinders are likely to require helium atoms to diffuse longer distances through bulk solid to reach a gas–solid interface. The equilibration time of ^{4}He concentration between the solid and gas phases will therefore likely increase.

4.1 EXPERIMENTAL APPROACH

Literature values for diffusivity and solubility of helium in solid UF_6 do not appear to be available. Therefore, an experiment was devised to make at least a first attempt at addressing these issues.

A stainless-steel U-tube, shown in Figure 2, was filled with 92 g UF_6. The U-tube was warmed to 100°C and held upright while allowed to slowly cool. The goal was to form a solid plug of UF_6 in the bottom of the tube, but the resulting solid apparently formed cracks and voids during cooling, likely caused by stress due to small changes in density in the solid during cooling. A second approach was employed that passed UF_6 gas through the U-tube while the bottom 1 in. of the tube was held at 0°C in an ice bath until a plug formed that stopped the flow. Eventually the flow of gas completely stopped. The ice bath was then allowed to slowly come to room temperature while the system was checked periodically to ensure gas flow was still blocked. When the system reached room temperature (23°C), the UF_6 solid was calculated to occupy 13.15 cc (JC Anderson), which would fill an idealized cylinder with a height of 14.1 cm based on its inner diameter and if the solid was void-free.

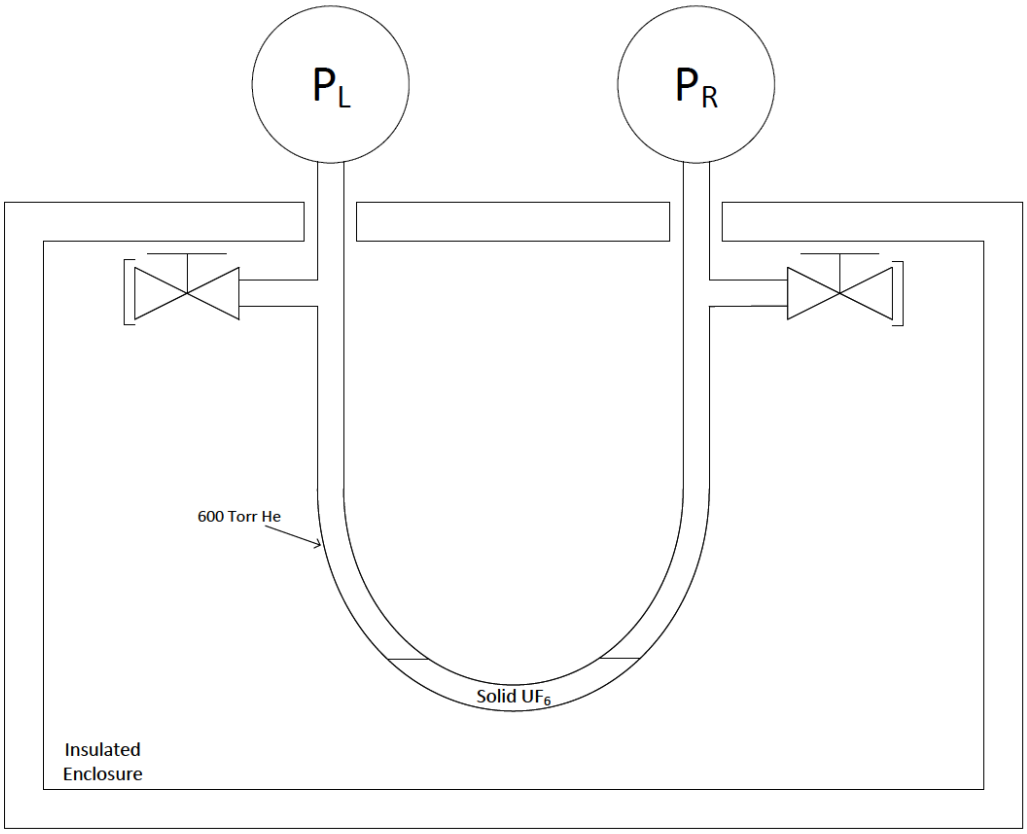

Figure 2. Apparatus to measure diffusivity of helium in solid UF_6.

The high-pressure side of the U-tube was briefly evacuated and then isolated while the other side was filled with a known pressure (~600 Torr) of helium. The low-pressure side was left as it was and assumed to be predominantly filled with UF_6 gas. The U-tube was transferred to an insulated vessel to try to maintain uniform temperature and minimize exposure to thermal cycling within the ambient room. The pressure was continuously monitored on both the high- and low-pressure sides using the pressure gauges, and the contact temperature was monitored using three thermocouples that were placed on the high- and low-pressure arms as well as the base of the U-tube. Once thermally stabilized, the system was left as it was for approximately 2 months.

Two derivative pressure parameters were also recorded, one the *sum* of the two pressures and the other the *difference* of the two pressures, as shown in Figure 3. The difference was particularly convenient because it alone was relatively free of pressure fluctuations brought on by slight temperature variations (not quite ± 1°C) that occurred from time to time even while inside the insulated vessel. The two direct pressure readings contain a component because of the UF_6 vapor pressure, which will change at a rate of about 7 Torr/°C at 23°C while helium would change at 2.03 Torr/°C at 23°C. Ideally, the changes in UF_6 vapor should subtract the vapor pressure on one side from that on the other, leaving only the residual helium partial pressure. The pressure values on each side of the plug were tracked over a 50 d period that represented the thermally stable period of the experiment. Early in the experimental run (12 h from noon to midnight on March 18, 2020) as the system was establishing equilibrium, considerably larger temperature and pressure variations occurred compared to later in the run; this period was therefore not incorporated into the data fit. Difference P_{DIF} and P_{HIGH} logs are shown in Figure 3. The vertical axes are on the same scale (although offset) and show the reduction in the data fluctuations afforded by the P_{DIF} variable as contrasted with the P_{HIGH} data.

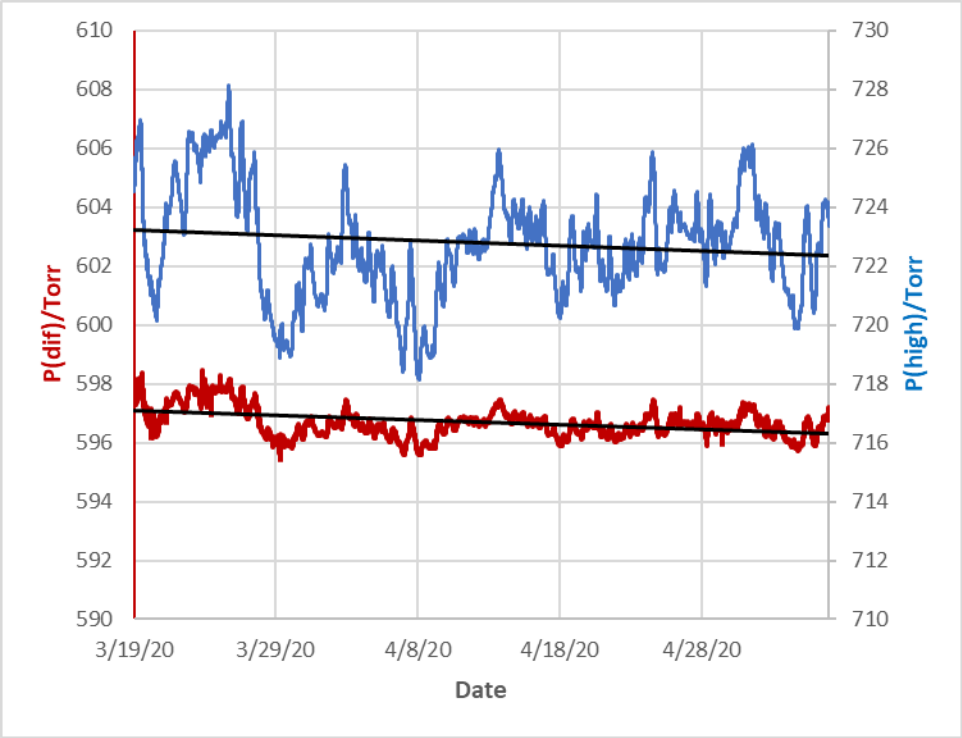

Figure 3. Data log of high-pressure side (blue) and pressure difference between two sides of plugged U-tube (dark red). The solid lines are the linear fits of P pressure over time.

Late in the experiment (beyond the time plotted in Figure 3), when it appeared that virtually nothing had been happening for 50 d, deliberate temperature excursions were performed. The U-tube was chilled to 18°C in stages, warmed to 25°C, and then quickly cooled to below 18°C. The pressure suddenly (within one 5 min data recording interval) equilibrated between the two sides of the tube during the rapid cooling cycle, which is assumed to indicate that a leak path had been opened by thermal contraction of the solid UF_6. For purposes of examining diffusivity, we will concentrate on the middle portion of the data log when the temperature was the most stable, namely the time interval starting 12 h into the experiment, over the 50 d between midnight March 19, 2020, and midnight May 7, 2020.
Three of the pressure logs, P_{HIGH}, P_{LOW}, and P_{DIF}, were subjected to a linear regression fit over this stable period and detected a change in pressure reading from start to finish of the stable period. The fitted start-to-finish pressure changes are listed in Table 2 and are also depicted in Figure 3 for two of the pressure fits (the black trendlines). Also listed in the table are the results of the Excel function STEYX (i.e., standard error for *y* evaluated at *x*), which, roughly speaking, gives the standard error of the fit relative to the data. For only the P_{DIF} parameter was the start-to-finish decline in pressure of greater magnitude than the estimated error. The P_{HIGH} value gave a reasonable and consistent decline but had a standard error that was twice its value. The P_{LOW} value declined slightly, whereas logically it should have remained constant or risen.

Table 2. Pressure and pressure change regression fits, 0 to 50 d

	P (day 0)	P (day 50)	50 d decline	STEYX (p, t)
	Torr	Torr	Torr	Torr
P_{HIGH}	723.22	722.36	0.86	± 1.91
P_{DIF}	597.11	596.29	0.82	± 0.48
P_{LOW}	126.11	126.07	0.04	± 1.44

Note: Values shown above display one or two statistically insignificant digits.

The expected behavior of P_{DIF} is as follows: If an amount, X, of helium is lost from the high-pressure side to solubility in the solid UF_6, P_{DIF} will decline by X. If, however, the same amount passes from the high side through the solid plug into the gas space on the low side, then P_{DIF} will decline by 2X. Ideally, we could separate loss to solubility from loss to transport *through* the barrier using a combination of P_{DIF} with P_{HIGH} or P_{LOW}, but the errors are too great in the last two pressure values to make such an attempt meaningful.

4.2 DIFFUSIVITY DISCUSSION

This experiment was designed to yield noticeable results if diffusion was of a magnitude that would be significant in the age dating operation. The experimental outcome, however, showed barely any indication of gas transport into or through the UF_6 plug during the 7 week constant-temperature period of the experiments. Indeed, from the statistics, it is not entirely improbable that the detection of a decline was simply due to random (or undetected systematic) drift. Nevertheless, we will proceed to see what can be made of the small decline apparently observed, keeping in mind that any resulting values for D or H^{CC} should possibly be treated not as definite values but as limits.

From the small change observed in P_{DIF}, a value for D *could* be derived if a reliable value for H^{CC} was available and valid at the temperature of the experiment. Unfortunately, the H^{CC} value measured in the section on solid solubility was for a temperature of nominally 77 K (or possibly deriving from solubility at a somewhat warmer, if still cryogenic, temperature within the cold trap).

Investigation of the range of diffusivities and solubilities consistent with the experimental observations was undertaken using a finite element model of the experimental apparatus that simulated helium absorption into the solid UF_6, diffusion along the length of the solid plug and desorption from the low-side surface of the plug. (See APPENDIX B.)

In modeling P_{DIF} decline, diffusivity and solubility proved to be correlated. That is, the model produced a range of data pairs (D, H^{CC}), all of which yielded model results that reproduced the experimental 50 d decline in P_{DIF}. For example, the data pair where D was 2.47×10^{-5} cm^2/s and H^{CC} was 2.23×10^{-3} provided a good match to the experimental pressure decline. This data pair was generated by fixing the H^{CC} value found in the solid solubility experiment (despite it being for a temperature far from 23°C) and then finding the value of D that best reproduced the 0.8 Torr decline in P_{DIF} observed experimentally.

However, a whole series of data pairs of D and H^{CC} reproduced the same 0.8 Torr, 50 d decline. Figure 4 plots H^{CC} versus D for helium in solid UF_6 and in selected organic and perfluoro polymers.

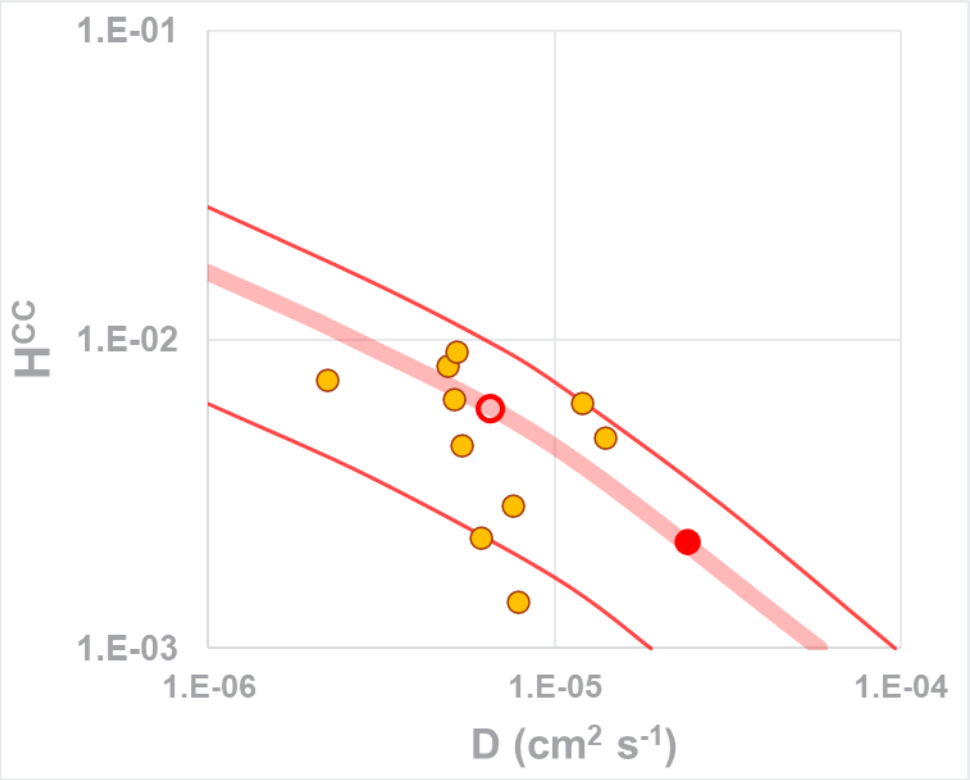

Figure 4. Correlation of helium diffusivity and solubility in solid UF_6 and several covalent non-polar polymers measured near room temperature. The thick pink line maps helium in UF_6 values for D and H^{CC}, and the thin red lines are the best fits to PDIF ± 1 standard deviation for helium in UF_6. The solid red point uses H^{CC} found at 77 K with D matching the observed experimental pressure decline, while the open red point selects a D-versus-H^{CC} pair that lies on the best-fit line and is also amid the helium–polymer data point cluster.

The series of D and H^{CC} pairs that reproduced the 0.8 Torr P_{DIF} decline are depicted by the wide pink line in Figure 4. The outlying thin red lines are data pairs that reproduced a decline of 0.8 ± 0.5 Torr (i.e., ± one standard deviation in the fit). Two red circles are plotted on the "best match." The solid circle plots the (D, H^{CC}) values mentioned above. That solubility is the value found at a cryogenic temperature, but the appropriate room temperature value is almost surely higher, though how much is difficult to say.

The open red circle likewise is on the "best match" line but was deliberately (and subjectively) placed roughly in the middle of the cluster of orange circles (which represent literature values for D and H^{CC} for several common hydrocarbon and fluorocarbon polymers, listed in Table A-2.). The values for the red open circle are D of 6.8×10^{-6} cm^2/s and H^{CC} of 6.0×10^{-3}.

We would expect the true room temperature values for helium solubility and diffusivity in solid UF_6 to lie in the vicinity of this data pair, likely within the one-standard-deviation lines and probably within the neighborhood of the polymer data points. The argument from the present experimental data is weak due to the minimal change in pressure, and the argument of similarity to the polymer properties is subjective. The true values could well lie lower than this data point but could not lie very much higher because such values would have inevitably led to an unmistakable pressure decline in P_{DIF}. In that sense, the D and H^{CC} values suggested here can be treated as upper limits on their true values.

A few additional points should be made regarding these values. First, considering the experiment reported here was a one-time experiment, random or systematic errors in the experiment could have conspired to produce the observed slight pressure decline for reasons other than permeation of helium into and through the UF_6 plug. Second, the diffusion barrier was experimentally 14 cm in length at most and has been treated as 14 cm throughout the data analysis, modeling, and discussion in this report. The effective length, however, may have been shorter if there were cracks or voids in the solid. Given the difficulty in forming a plug, it is expected that these formations are common, which would mean that the gas did not fully penetrate the 14 cm barrier due to these cracks and voids and therefore had a much more rapid transport of gas along the length. If that was the case, the effective length of the barrier would be smaller, and the true value of D would be lower than we have calculated. Again, this implies that the apparent D reported here is an upper limit on its true value.

Implications for age dating process: When the diffusion barrier is very thin (a small quantity of solid spread over large area) or when much of the solid volume is found in an amalgam of porous, perhaps needle-like crystals (as can happen in low temperature UF_6 cold trapping), diffusion should be able to rapidly equilibrate the solid and gas concentrations. In contrast, if there are many centimeters of fully dense solid between the interior and the surface of a mass of UF_6 solid, diffusional exchange between solid and gas will be slow. If this is the case in a large UF_6 cylinder, we might expect the helium equilibration time between the solid and gas to be quite long.

As discussed earlier, the end of this diffusion experiment came when the temperature was cycled up and down by a few degrees. On the second downward cycle, the pressure between the two sides suddenly equilibrated, completing the pressure equilibration within a few minutes (on the order of a single 5-min data recording interval) as shown in Figure 5 below, beginning during a approximately 6°C drop in temperature. Cylinders subject to warming or cooling are often heard to be "crackling," which may occur during temperature change events (e.g., during diurnal temperature changes during outdoor storage or during cooling after liquefaction). The presence of cracks caused by thermal excursions could be expected to greatly speed up equilibration of helium within whatever portion of the solid UF_6 is affected by this phenomenon.

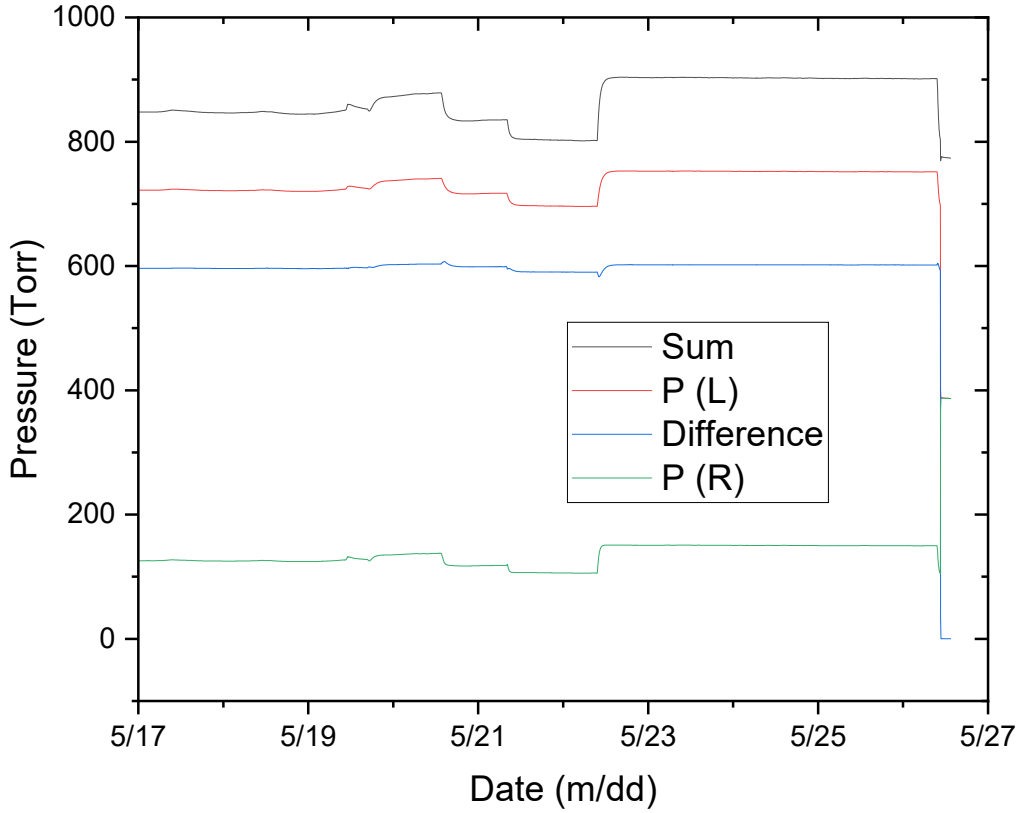
1000
800
600
400
200
0
Pressure (Torr)
5/17
5/19
5/21
5/23
5/25
5/27
Date (m/dd)
Sum
P (L)
Difference
P (R)

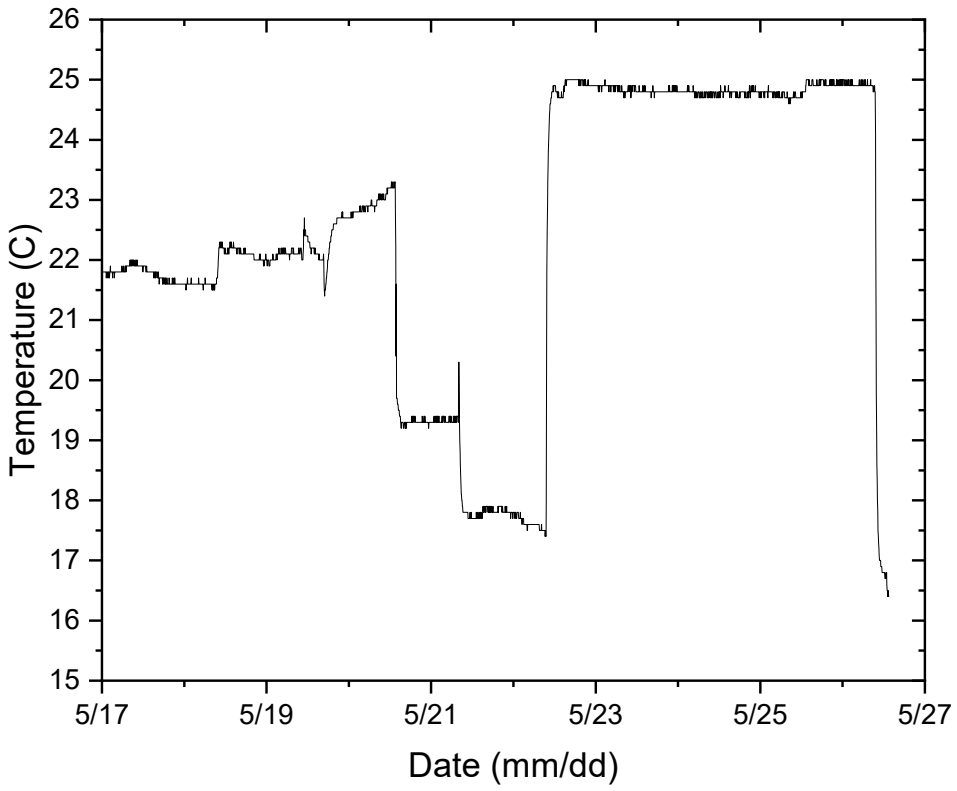

Figure 5. Pressure and temperature data from the plugged U-tube.

In addition to thermally induced cracking, the radioactivity of uranium itself can damage the structure of UF_6 solid on a molecular level. A typical alpha particle and the recoiling daughter nucleus can create a damage track involving on the order of 30,000 UF_6 molecules (EC Ramon). While still not a large fraction of the UF_6, especially for low assays, the damage tracks might be speculated to enhance the diffusivity of helium in the solid.

Overall, the D and H^{CC} values found in this work (even with their considerable uncertainty) suggest that, if not disrupted, helium embedded in solid UF_6 more than a few centimeters from a surface may take weeks or months to equilibrate with the headspace gas. The surface, however, includes not only the macroscopic bulk surface but also the cracks in the crystalline mass of UF_6 if those cracks are in communication with the headspace.

5. ATMOSPHERIC NOBLE GAS BIAS

One theorized source of error in the ^4He measurement is related to the method used to correct for its presence in the system as a result of air ingress. The correction relies on the well-established ratios of noble gases in atmospheric air. The amount of air in the system is calculated using the measured quantities of argon and krypton isotopes in the system, and then the ^4He contribution from air is calculated based on the natural molar ratios. If there is any selective partitioning of noble gases into UF_6, then the use of atmospheric molar ratios of noble gases to calculate the ^4He contribution from air would be biased.

5.1 EXPERIMENTAL

Two 75 cc sample bottles were prepared with 85 g UF_6 each, and a third was used empty. A known amount (~100 Torr) of ultra zero air (UZair) was added to each bottle. (Note that UZair is a grade of compressed, purified air with very low water and organic content.) One of the UF_6-containing bottles was heated to melt the UF_6, inverted several times to equilibrate the gas and liquid, and then allowed to cool back to room temperature. The three samples then represented air, air over solid UF_6, and air that had been in contact with liquid UF_6. Subsamples of each sample bottle's headspace gas were then analyzed on the age dating loop. Each sample was analyzed multiple times, and the average between the measurements was used. Additionally, two measurements were made of UZair that had been introduced into the sample manifold to account for any impacts by this system. Finally, two measurements of ambient air were also taken using an air pipette (AP). One measurement analyzed the AP directly, while the second collected the AP sample and processed it through the manifold to account for any process impacts.

5.2 RESULTS ON ATMOSPHERIC BIAS OF NOBLE GASES

The results of that analysis are shown in Figure 6, which depicts the abundance of three other isotopes as a ratio to ^{36}Ar. Argon and krypton isotopes show no bias among the gas sources or processing methods. Helium appears to have some difference between UZair (compressed gas cylinder) and AP (ambient) sources that may be an artifact of the process used to generate the compressed gas. The helium ratios for all UZair are within the statistical error (1 standard deviation) and so are considered equivalent. The AP and processed AP samples overlap at 2 standard deviations and therefore are considered equivalent. These results suggest that neither contact with solid or liquid UF_6 nor the processing conditions had an impact on the ratios of noble gases and that small differences, as observed between different air sources, would have been discernable.

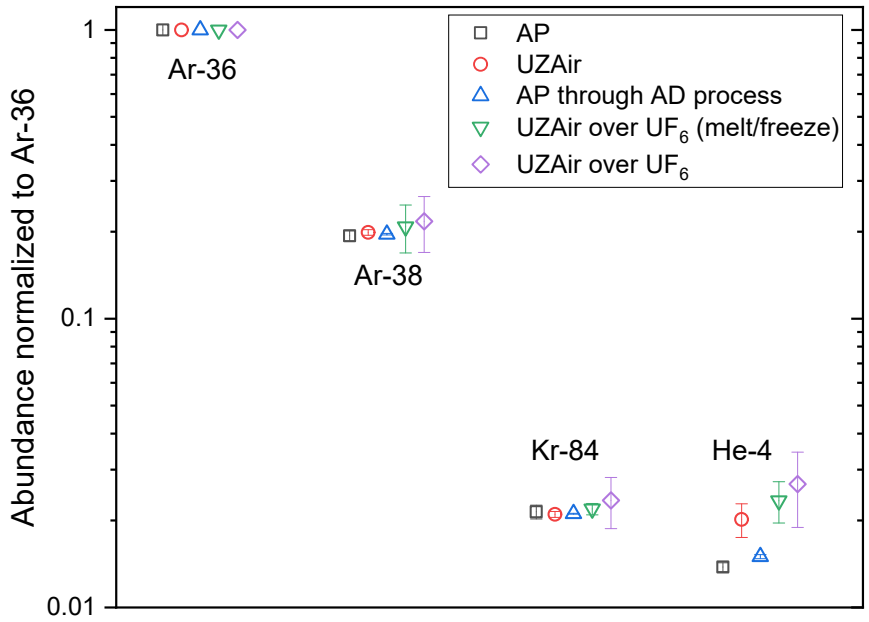

Figure 6. Noble gas measurements for ultra zero air over UF_6 plus several controls. Values are ratioed against the ^{36}Ar content, and the error bars are 1 standard deviation of the average.

6. ATMOSPHERIC HELIUM CHEMICAL TRAP BIAS

The fieldable sampling cart is designed with multiple approximately 13 L alumina traps to allow the collection of large volumes of UF_6 from many cylinders (GA Fugate). These traps are significantly larger than the chemical traps used on a laboratory scale and raised some concern that the preparation might have led to trapped helium that could have impacted measurements. The alumina traps were prepared by passing large volumes of dry compressed air through the heated trap material. This process could have allowed the more mobile helium to be concentrated in the microporous structure of the alumina. While it was not obvious that any back-streaming of helium from the traps into the active portion of the manifold had occurred, a field study at Paducah demonstrated excess helium in the first sample followed by the excess gas being reduced in each additional sample (Singleton, Stephenson and Beaumont). While there was no obvious route for this possible contamination to have impacted the work, the curious observed data suggested that this possibility should be eliminated as a potential concern.

6.1 EXPERIMENTAL

The activated alumina used in this experiment was prepared following the same procedure used to prepare the chemical traps that were part of the field exercise at the Paducah DUF6 facility (Singleton, Stephenson and Beaumont). Laboratory air (<2% relative humidity) was flowed over the 13 L activated alumina chemical trap while the trap was heated to a surface temperature of ~300°C using heat tape. This configuration was maintained for several hours until the exhaust gas was observed to be dry using a relative humidity gauge. The trap was then allowed to cool under a continuous flow of laboratory air. Once the trap reached room temperature, it was isolated. The trap used for this experiment had been isolated for a little over a year after the drying process was complete. For this test, its headspace gas was sampled and then run through the age dating process, yielding mass spectroscopy compositions for four noble gas isotopes. Additional samples of ambient air collected with the AP and an AP sample processed through the manifold were run through the age dating process to ensure the AP did not impart an effect.

6.2 AIR SAMPLING RESULTS

The results and the values as ratios to ^{36}Ar are shown in Figure 7, with each value representing the average of multiple measurements. The error bars show 1 standard deviation. All three gas samples appear almost identical to the composition of the four isotopes measured. This fact appears to rule out the alumina traps as a source of excess helium and demonstrates that the chemical trap should not bias ^{4}He measurements.

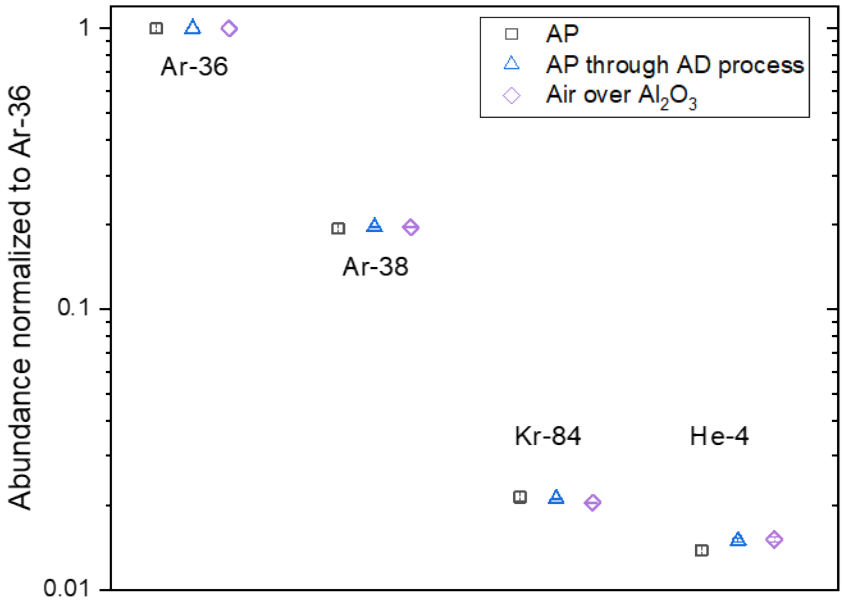

Figure 7. Air sampling results for a prepared, stored chemical trap compared to the air pipette samples taken directly from room air and room air run through the age dating gas procedure. Values are ratioed against the ^{36}Ar content, and the error bars are 1 standard deviation of the average.

7. CONCLUSION

Helium bias from extraneous sources: The age dating process as implemented uses a calibration and correction scheme involving measurement of one krypton and two agron isotopes for removing the contribution of atmospheric helium from the measurement. If differential retention or loss of any of the four isotopes (including helium) occurs within the process, the correction could bias the result. Two locations of potential holdup are within the solid UF_6 itself or within a high-surface-area chemical trap. Experimentally, no bias was observed for either.

Solubility of helium in liquid UF_6: A solubility constant for helium in liquid UF_6 at 100°C was determined experimentally. In terms of the dimensionless Henry's law constant, its value is $H^{CC} = 3.10\%$. This value implies that *some* helium could be carried into a cylinder being filled with liquid UF_6, but the gas phase of the source UF_6 would be some 32 times as concentrated as the liquid filling the new cylinder. An additional point is that the solubility value listed here lies within the range of values for helium solubility in several non-polar organic liquids.

Solubility of helium in solid UF_6: Solid solubility at, nominally, 77 K was determined to have a Henry's law constant of $H^{CC} = 0.223\%$. Considerable uncertainty exists in the effective temperature of the desublimation of UF_6 and sequestering of helium into the solid, which in turn affects the calculation of H^{CC}. An upper limit estimate of the cold-trapping effective temperature is 190 K, which leads to a value of $H^{CC} = 0.5\%$. Further constraints can be put on the solubility at room temperature from the results of the experiment on helium diffusion through a solid UF_6 plug. All these values are about an order of magnitude lower than the liquid solubility. Furthermore, they lie within the range of values for helium solubilities in several non-polar, covalent organic polymers. Finally, the solubilities listed here all indicate that, at equilibrium, less than 1% of the helium in a full UF_6 cylinder will be dissolved in UF_6; the balance will be in the headspace, accessible to the age dating process.

Diffusion of helium through solid UF_6: The plugged U-tube diffusion experiment demonstrated that helium diffusion through UF_6 is not rapid because a plug as thick as 14 cm (and possibly somewhat less if imperfections are present in the solid) will pass less than 1 Torr of 600 Torr in 50 d into and through the plug.

Looking into the U-tube in more detail, it was determined that limits could be put on the values for diffusivity and solubility of helium in room-temperature solid UF_6. The values that reproduce the (almost nil) observation of pressure change are, however, correlated in such a way that the specific values of these properties cannot be elucidated independent of one another from this experiment. That said, values are proposed that are, at worst, upper limits to these parameters.

Helium is, however, known to diffuse from solid UF_6 on a dimensional scale close to that of the plugged U-tube experiment. In small UF_6 cylinders, we have empirically observed that radiogenic helium is virtually all accessible on a timescale far less than the 50 d in the U-tube experiment. That is not, apparently, due to diffusion through thick, undisrupted solid UF_6, though. It could be aided by the presence of cracks or other imperfections in the solid; it could be that the solid UF_6 in a small cylinder is typically a thin, high surface area material less than a cm thick; or it could be that radiation damage allows enhanced mobility, especially in more enriched samples.

For large cylinders, we have no real proof that helium generated in the bulk solid is largely accessible to the headspace. One would have to imagine cracks going all the way to the bottom of the mass of the UF_6 solid and through up to a meter of solid UF_6 for the solid to be in good communication with the gas space. Sounds of cracking and snapping are heard coming from cylinders that are changing temperature (e.g., during outdoor storage when the temperature changes due to weather changes or during simple day-to-night changes), though. That implies some degree of acceleration of helium transport in cylinders subject to temperature swings during storage. Additionally, formation of a true plugged UF_6 solid proved to be difficult to fabricate and required flowing condensation to fill pores.

We also observed a sudden pressure equilibration upon a 7°C temperature change. Deliberately inducing a 10°C temperature change could promote helium equilibration between solid and gas phases by shortening the distance from the interior of the solid to the solid–gas interface. It might also aid in clearing a plugged U-tube or pipe by opening a path to promote flow.

8. REFERENCES

B Flaconneche, J Martin, MH Klopffer. "Permeability, diffusion and solubility of gases in polyethylene, polyamide 11 and poly (vinylidene fluoride)." *Oil Gas Sci Technol* (2001): 261-278.

CL Wearner, JA Behr, A Gorelov. "PCTFE as a solution to birefringence in atom trap viewports." *Rev Sci Instr* (2014): 113106.

Clever, HL, ed. *Solubility Data Series*. Vols. 1 Helium and Neon - gas solubilities. New York: Pergamon Press, 1979.

EC Ramon, LE Borg, LD Trowbridge, DW Simmons. *Uranium hexafluoride studies: final technical report on cylinder heels*. LLNL-TR-4000692. Livermore: LLNL, 2008.

GA Fugate, H Jennings, LR Martin, J Richards, D Simmons, M Singleton, L Trowbridge. *Design of fieldable head space manifold*. ORNL/SPR-2019/1249. Oak Ridge: ORNL, 2019.

Henry's Law. n.d. 24 10 2022. <https://en.wikipedia.org/w/index.php?title=Henry%27s_Law&oldid=1118048194>.

J Richards, LT Trobridge, DW Simmons, HJ Jennings, CP Boring, LR Martin, GA Fugate, P Stephenson, WC Beaumont, WS Cassata, MJ Singleton. "In-field collection and analysis of uranium hexafluoride cylinder head space gas for the evaluation of fill date." *61st INMM Annual Meeting*. Baltimore: INMM, 2020.

JC Anderson, CP Kerr, WR Williams. *Correlation of the thermophysical properties of uranium hexafluoride over a wide range of temperature and pressure*. ORNL/ENG/TM-51. Oak Ridge: ORNL, 1994.

"List of cooling baths." n.d. *WikiPedia.* 23 7 2023. <https://en.wikipedia.org/wiki/List_of_cooling_baths>.

Singleton, M, et al. *Helium age dating of UF6 sample cylinders*. LLNL-TR-756167. Livermore: LLNL, 2018.

—. *U-He ages of UF6 cylinders: 2019 Paducah campaign*. LLNL-TR-833274. Livermore: LLNL, 2023.

SJ Hansen, MD Rogers, ed. *The UF6 Manual: good handling practices for uranium hexafluoride*. USEC-651, Rev 9. Bethesda: USEC Corp., 2006.

USEC, ed. *Uranium Hexafluoride: a manual of good handling practices*. USEC-651, Rev 7. Bethesda: USEC, 1995.

APPENDIX A. SOLUBILITY AND DIFFUSIVITY LITERATURE

The most fundamental questions examined in this report are (1) what is the helium solubility in solid and in liquid UF_6? and (2) what is the He diffusivity in solid UF_6? Unfortunately, other than our own work, we are not aware of any direct data on this question. The very symmetrical, non-polar nature of the UF_6 molecule may lead it to behave similarly to other covalent, non-polar solids and liquids.

HELIUM SOLUBILITY IN LIQUIDS

For reference, values for helium solubility in several simple hydrocarbon and perfluorocarbon liquids are listed in Table A-1.

Table A-1. Values for helium solubility (converted to and listed as H^{CC}) for several non-polar hydrocarbon and fluorocarbon liquids. Values range from 2.1% to 5.5% for simple hydrocarbons. The three fluorocarbons overlap this range with the highest having a value of 9.2%.

Liquid	Hcc	T (°C)	Source
pentane	5.50%	25	(Clever)
hexane	4.79%	25	(Clever)
heptane	4.13%	25	(Clever)
octane	3.52%	25	(Clever)
nonane	3.28%	25	(Clever)
decane	2.98%	25	(Clever)
dodecane	2.40%	25	(Clever)
benzene	2.10%	25	(Clever)
PF benzene	4.50%	24	(Clever)
cyclo-C_7F_{14}	8.65%	16	(Clever)
C_7F_{16}	9.20%	22	(Clever)
UF_6(liq)	3.10%	100	this work

For comparison, the solubility of helium in liquid UF_6 at 100°C determined in this work is listed at the end of Table A-1. Absent any other data on UF_6, we might expect its value to resemble that of the fluorocarbons, but we find that the experimentally determined value falls below the three perfluorocarbons and within the hydrocarbon range. Furthermore, the UF_6 value is for a temperature of 100°C, whereas the other tabulated data are largely at or near room temperature. Where temperature dependence is available (and it is for all but UF_6 and pentane among the Table A-1 entries) (Clever), solubility increases with increasing temperature. UF_6 liquid would therefore likely have a lower solubility near its melting point.

HELIUM SOLUBILITY IN SOLIDS

Again, we did not find literature data on the solubility or diffusivity of helium in solid UF_6, but values are available for helium in a variety of non-polar organic polymers. A selection of these is listed in Table A-2. . The range of values for the dimensionless solubility constant H^{CC} falls into the tenths of a percent, which is to say approximately 10% of the solubility values for helium in the organic liquids listed in Table A-1. As with the liquids, those with some fluorocarbon character fall into the upper end of the range of helium in hydrocarbons.

Included for comparison at the end of the Table A-2. are two values of the solubility constant for helium in solid UF_6 from this present work. As with the helium-in-liquid value, both can be seen to fall within the range of values listed in Table A-2.

Table A-2. Literature values for solubility of helium in several non-polar organic solids

Solid	D $cm^2\ s^{-1}$	H^{CC}	P_e [a] scc cm $cm^{-2}\ s^{-1}\ atm^{-1}$	Reference	T °C	Notes
LDPE	1.20×10^{-5}	0.622%	6.48×10^{-8}	(B Flaconneche)	41	[b]
LDPE	1.40×10^{-5}	0.481%	5.88×10^{-8}	(B Flaconneche)	40	[b]
MDPE	5.10×10^{-6}	0.640%	2.84×10^{-8}	(B Flaconneche)	41	
HDPE	7.60×10^{-6}	0.291%	1.93×10^{-8}	(B Flaconneche)	41	[b]
HDPE	6.10×10^{-6}	0.229%	1.22×10^{-8}	(B Flaconneche)	41	[b]
HDPE	7.80×10^{-6}	0.142%	9.63×10^{-9}	(B Flaconneche)	41	[b]
PVF2	2.20×10^{-6}	0.742%	1.42×10^{-8}	(B Flaconneche)	41	
Nylon	5.40×10^{-6}	0.453%	2.13×10^{-8}	(B Flaconneche)	41	
Kel-F	4.90×10^{-6}	0.824%	3.70×10^{-8}	(CL Wearner)	room	
Viton	5.20×10^{-6}	0.911%	4.40×10^{-8}	(CL Wearner)	room	
UF_6(solid)	2.47×10^{-5}	0.223%	4.98×10^{-8}	this work	–196	[c]
UF_6(solid)	6.8×10^{-6}	0.6%	3.60×10^{-8}	this work	23	[c]

[a] Due to the units chosen for D, H^{CC}, and P_e, a temperature correction is required such that Pe = D and $H^{CC} = T_s / T_e$, where the units of T are in K and $T_s = 273.15$ K.
[b] Multiple low-density polyethylene and high-density polyethylene entries are from different preparation methods.
[c] Values for helium in UF_6 are from this work. The first entry uses experimental H^{CC} determined at approximately 77 K. The second entry uses values consistent with the experiment but forced to be like polymers.

HELIUM DIFFUSIVITY IN SOLID ORGANICS

Diffusivity, in units such as cm^2/s, describes the transport of a dissolved material (in this case helium) within a solid material (or non-convecting liquid) that is driven by a concentration gradient within the solid as calculated by

$$\frac{dn}{dt} = -DA\frac{DC_{sol}}{dZ},$$

where *dn/dt* is the quantity of the diffusing component (i.e., in moles helium per unit time), *D* is the diffusivity (i.e., in cm^2/s), *A* is the cross-sectional area perpendicular to the concentration gradient of the material through which the diffusion is taking place (i.e., cm^2), and dC_{sol}/dz is the concentration gradient of the solute (i.e., moles helium/$cm^3 \cdot cm$).

It is important to keep in mind that the diffusivity applies to the concentration *within* the solid and is not the same as the *permeability*, which is used to describe transport through a solid based on a difference in concentration or partial pressure *outside* the solid. The solubility and diffusivity constants both enter the permeability constant, P_e, a parameter often listed for thin barriers such as plastic films.

Table A-2. lists the diffusivity of helium in several organic polymers. Values span about an order of magnitude from the low 10^{-6} up to the low 10^{-5} cm^2/s.

Also listed in the table are the values estimated from the UF_6-plugged U-tube experiment. Both D values, with their associated solubility values, reproduced (in the finite element diffusion model described in APPENDIX B) the experimental outcome at the end of the stable portion of that helium diffusion experiment. One value used a measured but temperature-inappropriate value for the solubility, while the other reproduced the experimental outcome using values for D and H^{CC} chosen to lie among the hydrocarbon and fluorocarbon D, H^{CC} data pairs. (See Figure 4 and associated discussion.)

REFERENCES

Clever, HL, ed. *Solubility Data Series*. Vols. 1 Helium and Neon - gas solubilities. New York: Pergamon Press, 1979.

APPENDIX B. DIFFUSION MODEL

For the purposes of analyzing the results of the U-tube diffusion experiment, a simple numerical model was devised to simulate the transport of helium gas from the void space on one side of the U-tube through the solid UF_6 plug to the other U-tube leg's void space. To simplify the geometry, in the model the U-tube is treated as a straight tube with a plug of UF_6 in the center. The void spaces on either side of the UF_6 plug consist of a single cell matching the volume of the void space above the solid UF_6 surface in the U-tube. Transport of helium from (or to) the void space is treated by assuming that within an infinitesimal layer of solid UF_6 at the surface of the plug, dissolved helium is in equilibrium with the partial pressure in the adjacent gas space. The concentration of helium in the solid is calculated from the solubility constant H^{CC} (either obtained experimentally or simply postulated). D is likewise postulated.

The solid plug is modeled as 14 cells, each being 1 cm in length. (The calculated volume of UF_6 used in the U-tube happened to be very nearly the tube's cross-sectional area times 14 cm). Diffusion of UF_6 within the solid is calculated across each cell interface per

$$\frac{dn_{i,i+1}}{dt} = -\frac{D(C_i - C_{i+1})\,A}{L},$$

where $dn_{i,i+1}/dt$ is the number of moles of helium crossing the boundary between cell i and $i+1$ per unit time, D is the diffusion constant for helium in solid UF_6, C_i is the concentration of helium in cell i, A is the cross-sectional area of the tube (0.9369 cm^2), and L is the distance between cell centers (1 cm, except for the first and last cell-to-surface-layer distance, which is taken as 0.5 cm). A pictorial schematic of the geometry used in shown Figure B-1.

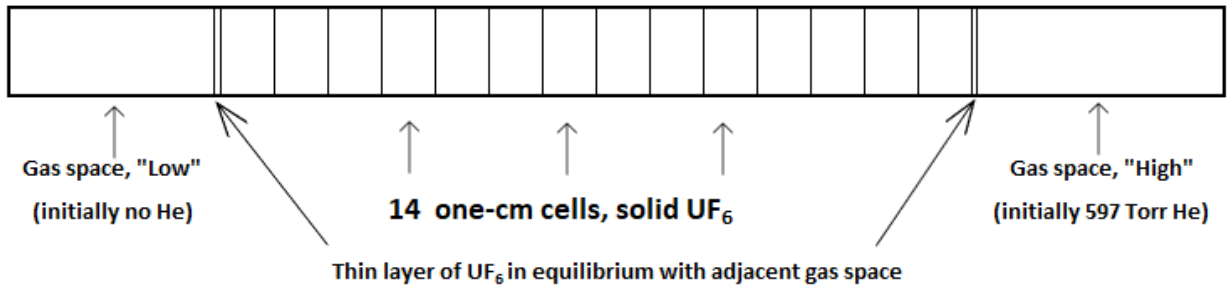

Figure B-1. Idealized schematic showing cell and regions used in the diffusion model.

The initial conditions for the model were specified to match the experimental starting conditions: 597.11 Torr helium in the "high side" gas space, no helium in the "low side" gas space or in any of the solid UF_6 cells. An iterative series of calculations was undertaken using specified time increments. For each time interval, the transport values were calculated for each cell boundary (i to i+1 in the above equation). Then the helium inventory of each cell was calculated by adding the contributions from its two adjacent boundaries (e.g., i-1 to i and i to i+1). Transport from the first and last cell to the thin surface layer added or withdrew helium from the adjacent gas space. After adjustment of the inventory, the new set of concentrations and gas space partial pressures became the starting conditions for the next time interval.

Time increments were adjusted to avoid erratic model behavior, short intervals (5 s) being required early on when the concentration gradients in the solid were at their largest. Later in the simulation, longer time intervals (1 h) were used. The model was run for a total elapsed time matching the relatively stable portion of the actual experiment, 50 d.

Helium migration in the model depends primarily on the values for H^{CC} and D and the initial quantity of helium in the high-pressure side of the tube. The initial partial pressure of helium was taken as 597 Torr, the value determined by extrapolating the experimental P_{DIF} back to t = 0. H^{CC} and D are input parameters and may be freely specified for a given model run. In some cases, the "known" value of H^{CC} was specified to be 0.223%, which is the solubility constant experimentally found in the solid UF_6 solubility experiment reported elsewhere in this work. That value was known to be inappropriate in that it was determined at a temperature well below the 23°C U-tube experiment but was the only specific value at hand and left D as the single input parameter.

To deduce the best-match value of diffusivity, D was varied until the 50 d drop in P_{DIF} in the model output matched the 50 d value in the experimental data log. Due to unsteadiness in the pressure value, the linear fit to the 50 d value was used as the experimental target result, namely −0.82 ± 0.5 Torr. (See Table 2 in the main body of this report.)

The finite element model was run for several scenarios with the value of D, and sometimes H^{CC}, taken as adjustable input parameters. Results and parameters for several scenarios are summarized in Table B-1.

Table B-1. Finite element diffusivity model emulating U-tube helium transport experiment at 50 d with scenario results matching P_{DIF} decline for several assumptions

		[0] (Expt)	[1]	[2]	[3]	[4]
$H^{cc[a][b]}$ =		0.223%	0.223%	0.60%	0.30%	0.85%
$D^{[b]}$ =	cm^2/s		2.47E-05	6.80E-06	4.60E-06	8.30E-06
P_{DIF} (0 d)	Torr	597.11	597.11	597.11	597.11	597.11
P_{DIF} (50 d)	Torr	596.29 ± 0.48	596.29	596.29	596.79	595.79
delta P_{HIGH} (0–50 d)	Torr	–0.86 ± 1.91	–0.57	–0.76	–0.31	–1.20
delta P_{LOW} (0–50 d)	Torr	–0.04 ± 1.44	–0.25	0.05	0.01	0.12
delta P_{DIF} (0–50 d)	Torr	–0.82 ± 0.48	–0.82	–0.82	–0.32	–1.32
N(low)/N(lost)			43%	6.7%	2.3%	10%

[a] H^{CC} value used is that determined experimentally, nominally at 77 K.
[b] H^{CC} and D both adjusted to lie within helium-polymer (H^{CC}, D) cluster (see Figure 4).

The parameters listed for each scenario are values of H^{CC} and D used in that run: the P_{DIF} initial (0 d), final (50 d). Next are listed the change from 0 to 50 d in helium partial pressures on the high side and low side and the difference, P_{DIF}. It is this last value that the model sought to match by suitable adjustment of D and H^{CC}. The last row lists the ratio of the final quantity of helium *within* the low side gas space to the total loss of helium from the high side gas space (the balance being helium dissolved in the solid UF_6). Because of the large number of data points and their scatter, the values listed for pressures are taken from the regression-fitted values at t = 0 and t = 50 d rather than specific data values.

The first data column [0], shows the experimental values, where available, and lists the low-temperature H^{CC} value determined in the independent solid solubility experiment in this work.

The second data column (scenario [1]) shows a model run that used the value for D (2.47×10^{-5} cm^2/s) combined with the experimental H^{CC} value and best duplicated the experimental drop in P_{DIF}.

It was found that a set of correlated values of D and H^{CC} existed, all of which matched the 0.82 Torr experimental drop in P_{DIF}. This set of (D, H^{CC}) data pairs appear on the plot of H^{CC} versus D as a curved line. (See Figure 4 for further discussion. Scenario 1 values for D and H^{CC} are plotted in that figure as a solid red circle.)

The next scenario in Table B-1, [2], is a point chosen to both lie on the best fit line and in the midst of the cluster of data points for helium solubility and diffusivity in hydrocarbons shown in Figure 4.

The next two scenarios, [3] and [4], are points data sets (D, H^{CC}) like [2] but duplicate the experimental $P_{DIF} \pm 0.5$ Torr (i.e., ± 1 standard deviation in the fitted value of the final pressure drop). These points, like [2], are chosen to lie amid the cluster of polymer data points.

Absent further data, it appears likely (for quite subjective reasons) that the true value of H^{CC} and D for helium in solid UF_6 will lie between the ± 1 standard deviation lines plotted as thin red lines in Figure 4 and also within the cluster of helium–polymer points plotted in that figure.